Defect and Diffusion Forum
ISSN: 1662-9507, Vol. 434, pp 23-31
doi:10.4028/p-OqQTB1

Submitted: 2023-09-06
Revised: 2024-01-17
Accepted: 2024-02-16
Online: 2024-08-22

Study on Quantification of Correlation between Current Density and UV Irradiation Intensity, Leading to bar Shaped 1SSF Expansion

Yasuyuki Igarashi[1,a*], Kazumi Takano[1,b], Yohsuke Matsushita[1,c] and Takuya Morita[1,d]

[1]ITES Co., Ltd., 1-60 Kuribayashi, Otsu, Shiga 520-2151, Japan

[a]yiga@ites.co.jp, [b]kazumi_takano@ites.co.jp, [c]yohsuke_matsushita@ites.co.jp , [d]takuya_morita@ites.co.jp

Keywords: basal plane dislocation, single Shockley stacking fault, photoluminescence, UV irradiation, bipolar degradation, screening, recombination-enhanced dislocation glide.

Abstract. In 4H-SiC devices, the reliability issue of the bipolar degradation, which is caused by the nucleation and expansion of 1SSF (single Shockley stacking fault) defects originating from basal plane dislocations (BPDs), has not been completely eliminated. To avoid the reliability issue, in some device manufacturers is currently introduced so-called "burn-in" (accelerated current stress) screening operation, which is very time-consuming process which raises a total cost of production. While, the bipolar degradation is explained by the REDG (recombination-enhanced dislocation glide) mechanism, and the same degradation can be induced by UV (ultraviolet) irradiation. Using this property, we have been proposing a new screening method to detect latent defects with expanding to 1SSFs at an early stage of manufacturing. In order to bring this screening method to a practical level, it is essential to correlate the accelerated current stress with the UV irradiation quantitatively in terms of the effect of 1SSF expansion. We have attained some progress in an attempt to quantify this correlation and describe it in this paper.

Introduction

Currently, there are global calls for CO_2 reduction and efficient energy operation in order to build a sustainable society, and in the field of power electronics, the use of SiC as an alternative material to Si and its widespread use are accelerating in order to realize such a society as soon as possible. However, 4H-SiC devices, which are now widely used in products, have been found to have a reliability issue of so-called bipolar degradation for more than 20 years, but it has not yet been completely eliminated. The degradation is caused by the nucleation and expansion of a 1SSF [1], originating from BPD which exists in the epilayer or near the epilayer and the substrate (epi/sub) interface. The 1SSFs are expanded by the electron–hole recombination energy when excessive minority carriers are injected into the regions in the vicinity of the BPDs, which is called REDG (recombination-enhanced dislocation glide) mechanism [2].

Although recent process technology improvements have made it possible to convert more than 99% of BPDs to "benign" TEDs, which do not expand into SSFs, during the epitaxial growth process, further investigation has revealed that even converted BPDs expand to 1SSFs from a BPD-to-TED conversion point [3]. Then it has been proposed that high impurity concentration buffer layer is inserted between the drift layer and the substrate, in order to prevent minority carriers from reaching the conversion point [3, 4], but the expansion of 1SSF is not completely suppressed, especially in high current device applications [5], because the buffer layer cannot be made thick enough from a manufacturing cost perspective.

In addition, there is no commercialized in-line inspection system that can detect such “malignant” BPDs that are converted to TEDs at or below the epi/sub interface, but expand into 1SSFs, and therefore in some device manufacturers so-called "burn-in" screening is performed, in which the bipolar degradation is checked, chip by chip, by applying accelerated current stress for a certain period. This is a very time-consuming process which raises a total cost of production.

On the other hand, since it has been found that the expansion of 1SSF by the REDG mechanism can also be induced by UV (ultraviolet) irradiation [2], we have been proposing a new screening method to detect latent defects at an early stage of manufacturing, intending to replace the "burn-in" screening [6-8]. The aim of this method is, by utilizing UV irradiation, to enlarge and visualize latent defects that would cause bipolar degradation, but there is one important point to consider: the BPD-to-TED conversion point is wide vertically distributed from within the drift layer to just above the epi/sub interface or below the epi/sub interface. It has been reported that the more the current, the BPDs with the deeper conversion points would expand [9]. In other words, in device applications with lower current consumption, the BPDs with deeper conversion points would not expand. This is also true for UV screening. If the UV intensity is unnecessarily intense, even devices that would not show any degradation under low current application to be screened out, resulting in overkill (over-screening). The point is that the UV intensity during screening should be adjusted to suit the device application. Therefore, it is essential to know the quantitative correlation between UV intensity and current density condition with respect to 1SSF expansion.

To the authors' knowledge, few reports have addressed the quantitative correlation between current density and UV irradiation as a major topic. In this study, we have tried to quantify the correlation between them. We fabricated PiN diodes on a commercially available n-type 100 mm Φ 4H-SiC wafer, half of which are subjected to accelerated current stress and the other half was subjected to UV irradiation. 1SSF expansion rates for both cases were compared by tracking the position of the Si(g) core partial dislocation, the leading edge of 1SSF by UVPL (UV photoluminescence) observation and calculating its glide velocity for each case. The numerical relationship was, thus, derived via the glide velocities for 1SSF expansion between the applied current density and irradiance. Furthermore, the obtained data indicate that there is the point at which the glide velocity becomes zero, i.e., the "threshold" intensity below which 1SSF expansion doesn't occur at each stimulus (current density and UV irradiance), and therefore those "threshold" s were also estimated.

We also conducted the device simulation, in which the excess hole density under the threshold intensity of both the accelerated current stress and UV irradiation, was estimated. The simulation result showed that the hole density at the threshold of the accelerated current was close to the previous report [10], but in the case of UV irradiation, the estimated density was one or two digits higher than the report. We then examined the conditions of the simulation closely and found that, although our experiment used a pulsed laser source, the simulation treated it as a continuous wave, so we separately recalculated the hole density for the pulsed source by numerical analysis and confirmed that it is consistent with the reported value.

Experimental Results and Discussion

We fabricated PiN diodes on a commercially available n-type 100 mm Φ 4H-SiC wafer with a 4° off-cut angle. The structure of the PiN diode was formed by doping aluminum (3×10^{18} cm^{-3}) on the Si face of the epi wafer (buffer layer (0.5 μm, 1×10^{18} cm^{-3}), drift layer (5.4 μm, 5×10^{15} cm^{-3})) with a nickel electrode on the entire backside of the wafer. An aluminum electrode array of comb pattern (2mm square chip) was formed in half of the wafer for accelerated current stress, and the other half has no electrode pattern for UV irradiation stress, as shown in Fig. 1.

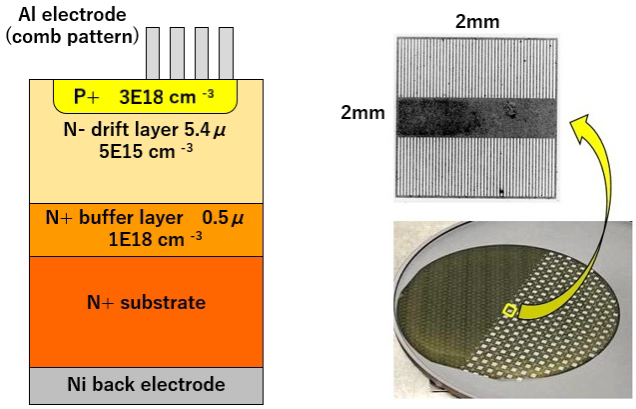

Fig. 1. Schematic diagram of the PiN diode and photos of aluminum electrode pattern on SiC Epi wafer

In accelerated current stress, the PiN diodes were subjected to seven levels of pulsed current (2 ms pulse width per 50 ms cycle (duty 4%)) from 250 to 400 A cm^{-2} in increments of 25 A cm^{-2}. The expansion was observed by UVPL (UV photoluminescence) at 420 nm BPF (band pass filter) as shown in Fig. 2 (a), and glide velocity was measured by observing the position of the leading edge of Si(g) core partial dislocation at each stress/irradiation intervals. While non-electrode patterned area of the same wafer was UV irradiated. The excitation source was 355 nm Nd: YAG-3HG (Yttrium Aluminum Garnet-third Harmonic Generation) pulsed laser with 10 ns pulse width per 20 μs cycle (duty 0.05%) and the energy per pulse was 211 μJ (at full power) measured at the surface of the specimen with beam diameter of 3 mmΦ. The laser power was controlled by the beam attenuator from 1% to 100% (full power) and in the experiment 1SSF expansion was observed by four levels of irradiation power (10%, 25%, 50%, 100%), and the glide velocity was measured in the same way as in current stress by UVPL observing the movement of the Si(g) core, as shown in Fig. 2 (b).

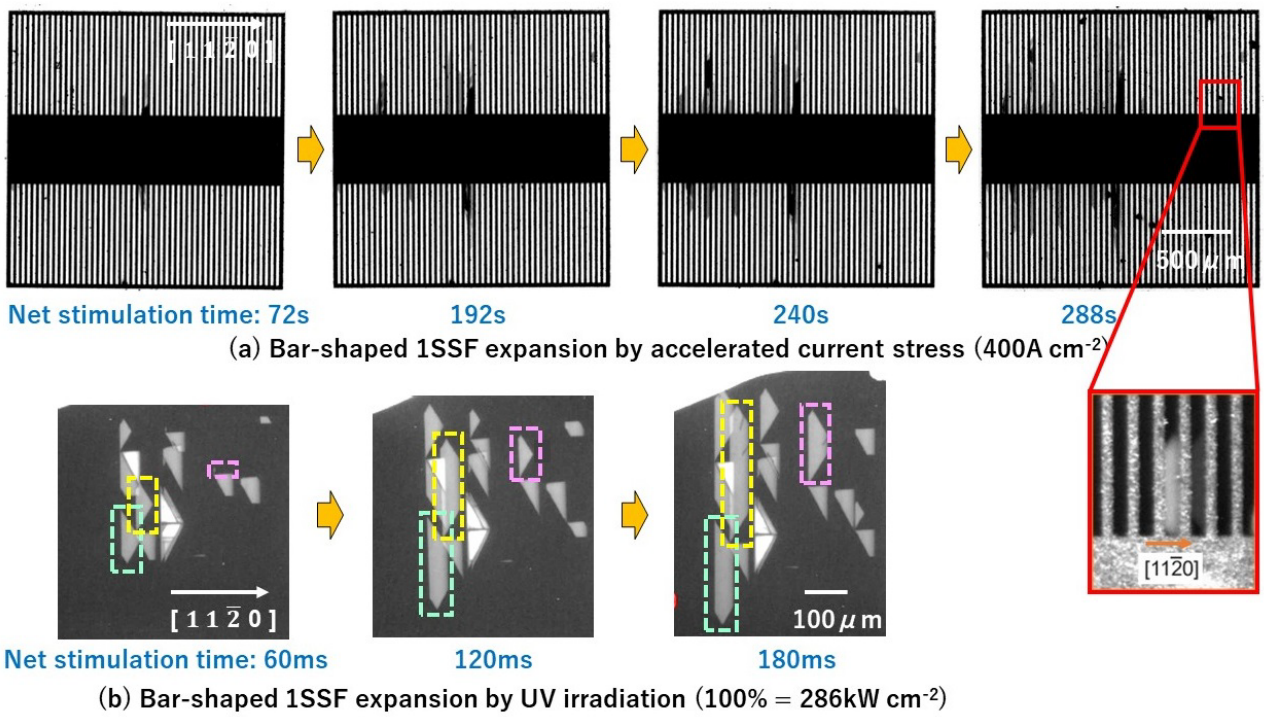

Fig. 2. Bar shaped 1SSF expansion under accelerated current stress (a) and UV irradiation (b).

The glide velocity was simply calculated by dividing the displacement (distance traveled) of the Si(g) core by the net stimulation time (current pulse width × frequency × applied time or laser pulse width × frequency × irradiation time), as shown in Fig. 3.

As a result, the measured glide velocities are shown by blue and red dots in Fig. 4. The number of measured bar shaped SSFs were 329 sites from 43 chips in accelerated current stress (Fig. 4 (a)) and 11 sites in UV irradiation stress (Fig. 4 (b)), respectively. As seen in the figure, even at the same current density or irradiation power, the measured glide velocities vary significantly, possibly due to various kinds of crystal defects which hinder the movement of the Si(g) core partials.

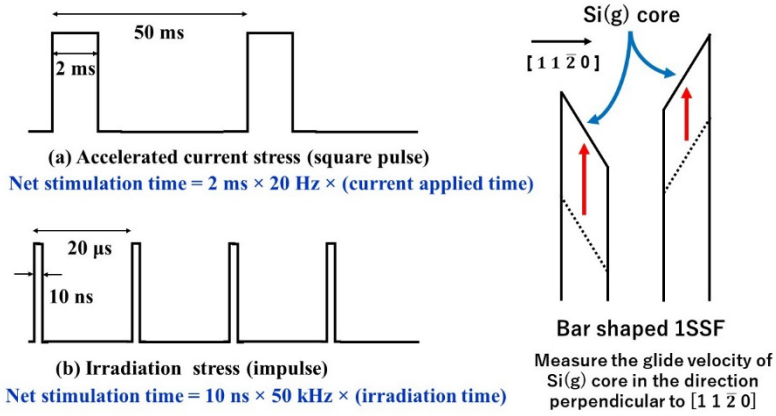

Fig. 3. Net stimulation time and glide velocity

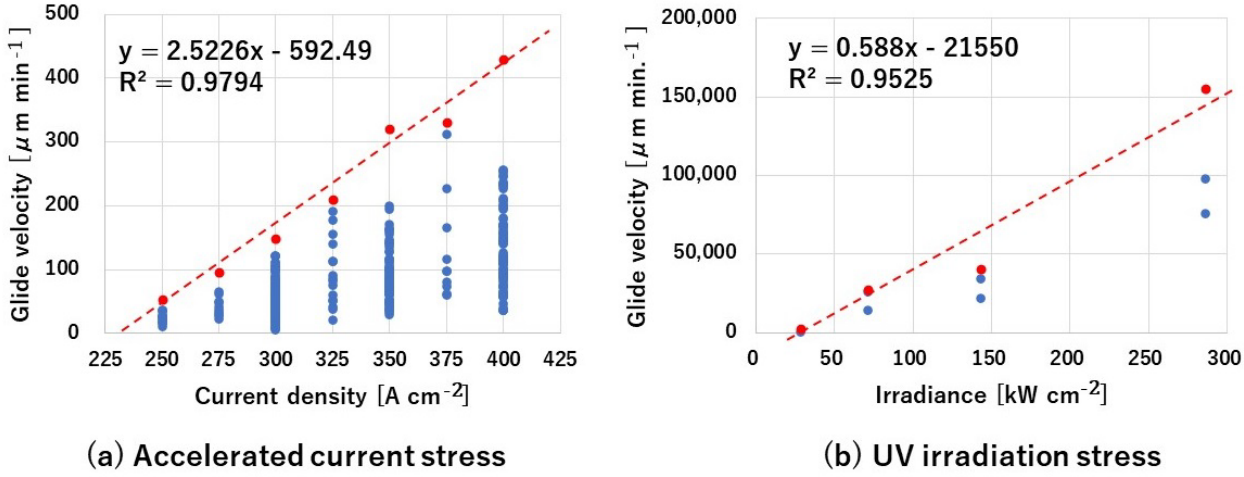

Fig. 4. Si(g) core glide velocity VS. stress intensity (Current density (a) and Irradiation power (b))

Since the purpose of the experiment was not to accurately measure the glide velocity itself but to see the correlation, it was thought to be a reasonable way to estimate the numerical relationship of glide velocity via a linear regression by picking up only the points with maximum speed at each stress level (red dots and red lines in Fig. 3 (a) and (b)), with the result of the glide velocity: v [µm s^{-1}] = 2.52(J [A cm^{-2}] – 235) = 0.588(E [W cm^{-2}] – 36650). The equation indicates that there is the point of zero velocity, i.e., a threshold for 1SSF to be generated/expanded, namely J_0 = 235 A cm^{-2} and E_0 = 36650 W cm^{-2}.

Since this equation is only valid for the one particular wafer used in the experiment, next we conducted the device simulation in order to make the above equation to be more general and versatile. It has been reported that the dislocation glide velocity is strongly dependent on the density of the injected excess holes [10] either by accelerated current stress or by UV irradiation. Therefore, using the one-dimensional device simulator, AFORS-HET, we estimated the hole density in case of the zero-expansion velocity obtained from our experiments and verified whether it is consistent with the previously reported threshold hole density of 1.6 to 2.5 × 10^{16} cm^{-3}[10]. The loss of UV light intensity was assumed to be based on the Lambert-Beer law and the absorption coefficient of 4H-SiC was set to 210 cm^{-1} (T=300K) at 355 nm [11]. As one of the major factors affecting the hole density especially in drift layer, recombination center of $Z_{1/2}$ defect was considered as the SRH (Shockley-Read-Hall) type recombination, and bimolecular (radiative) and Auger recombination were also considered. The bulk lifetime of the Epi drift layer was set to τ_{SRH} = 231 ns, by simply calculating from a recombination center with capture cross-sections for electrons and holes of 3.0 × 10^{-14} cm^2 and the $Z_{1/2}$ center density of 1.2 × 10^{13} cm^{-3}. Auger recombination rate of electrons/holes and bimolecular (radiative) recombination rate were assumed 7.00 × 10^{-31} cm^6 s^{-1} and 1.50 × 10^{-12} cm^3 s^{-1}, respectively

[12], but in the case of low impurity concentrations like the drift layer, the influence of these two parameters is little.

The laser power of specimen surface measured by laser power meter was 10.56 W (at full power), which corresponded to 286 kW cm^{-2} and the photon flux of 5.11×10^{23} cm^{-2} sec^{-1} during 10 ns pulse irradiation. Therefore, based on the above experimental results, the threshold of bar shaped 1SSF expansion, E_0=36650W cm^{-2} is 12.8% of full power, and accordingly the photon flux at the threshold is 6.55×10^{22} cm^{-2} sec^{-1}.

As a result, as shown in the Fig. 5, the estimated hole density under accelerated current stress (solid red line) was close to the reported value, but in the case of UV irradiation, the estimated concentration was 4×10^{17} to 9×10^{17} cm^{-3} (dashed blue line), one or two digits higher than the reported one. Taking into account that the spots irradiated with UV light were expected to be heated and therefore we ran the simulation again reflecting the temperature dependence of the absorption coefficient [13], but no significant change was observed. We then examined the conditions of the simulation closely and found that, although our experiment used a pulsed laser source, the simulation treated it as a continuous wave (CW), so we separately recalculated the hole density for the pulsed source by numerical analysis.

As described in the Appendix for details of the numerical analysis, the peak value of the hole density at the threshold of irradiance of E_0=36650W cm^{-2}, was estimated to be 1.3×10^{17} cm^{-3} (solid blue line), which is one digit lower than when simulated as CW, and is almost consistent with the simulated value at the accelerated current threshold and close to the previously reported value for 1SSF expansion threshold [10]. In addition, as illustrated in the Appendix Fig. A1, hole density decay curve indicates that the duration for the 1SSF expansion to progress (Si(g) core moving duration) is not irradiation time of 10 ns per pulse, but is estimated to be the time for the hole density to exceed the threshold value, 1.6×10^{16} to 2.5×10^{16} cm^{-3}, namely, 100 to 300 ns in case of the surface recombination velocity of 1000 to 10000 cm s^{-1}. Accordingly, the numerical correlation for that wafer used in the experiment should be modified as

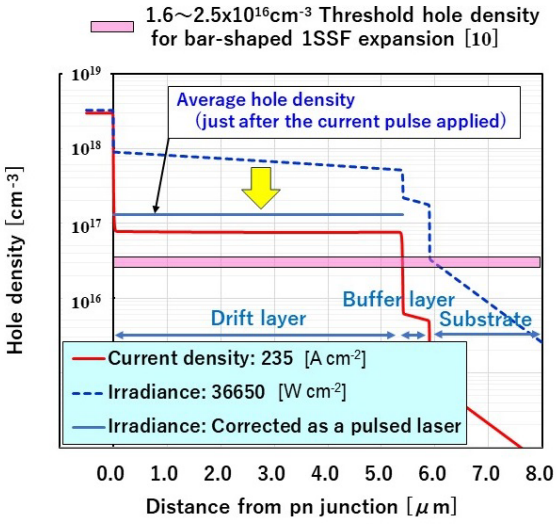

Fig. 5. Simulated depth profile of hole density

$$v = 2.52(J - 235) = 0.588\,k\,(E - 36650). \quad (1)$$

where

v: $Si(g)\ core\ glide\ velocity\ [\mu m\ s^{-1}]$

J : $current\ density\ \ [A\ cm^{-2}]$

E: $irradiance\ [W\ cm^{-2}]$

$k = 0.03\ to\ 0.1\ \ for\ S_0(surface\ recombination\ velocity)\ of\ 1000\ to\ 10000 cm/s.$

Summary

In this study, we attempted to quantify the correlation between current density and UV irradiance with respect to 1SSF expansion using the same wafer of commercially available n-type 100mmΦ 4H-SiC and obtained a simple correlation equation. In addition, from the experimental results, we estimated the respective thresholds of current density and UV irradiance at which bar shaped 1SSF begins to expand and calculated the excess hole density for those thresholds using one-dimensional device simulation and numerical analysis. The values were compared with previous literature and

confirmed to be consistent. The device parameters like impurity concentration in anode and drift layer, epi-layer thickness, Epi bulk carrier lifetime, and surface recombination velocity will affect the profile of excess hole density. As a next step, considering the difference in impact on the excess hole density between accelerated current stress and UV irradiation when such device parameters change, and reflecting the difference into the correlation equation, we expect that it will become more general and versatile.

Acknowledgments

This work was supported by 3-year project, METI "Monozukuri" R&D Support Grant Program for SMEs Grant Number JPJ005698 (METI=Ministry of Economy, Trade and Industry). The authors wish to thank Professor M. Kato at Nagoya Institute of Technology, and Associate Professor S. Harada at Nagoya University for their support as technical advisers in the project during this work.

Appendix. Estimation of hole density by pulsed UV laser irradiation

The hole density in the drift layer is estimated by a standard carrier diffusion model [14-18], in which the sample surface is irradiated with the pulsed laser light. The key parameter values used in the calculation are listed in Table 1.

Table 1. The parameters used in the calculation for excess hole density.

symbol	value	unit	description
D_a	5.64	$cm^2\ s^{-1}$	ambipolar diffusion coefficient
N_T	1.20×10^{13}	cm^{-3}	$Z_{1/2}$ density in drift Epi layer
σ	3.00×10^{-14}	cm^2	capture cross section
v_{th}	1.20×10^{7}	$cm\ s^{-1}$	hole thermal velocity
τ_b	2.31×10^{-7}	s	drift Epi bulk lifetime = $(\sigma\ v_{th}\ N_T)^{-1}$
d	5.4×10^{-4}	cm	drift Epi thickness
S_0	1,000～10,000	$cm\ s^{-1}$	surface recombination velocity
S_d	100	$cm\ s^{-1}$	interface recombination velocity of drift/buffer Epi
α	210	cm^{-1}	absorption coefficient of 355nm Nd:YAG laser [11]
N_0	6.83×10^{14}	cm^{-2}	number of photons per cm^2 per pulse at "threshold" intensity of 1SSF expansion
g_0	1.37×10^{17}	cm^{-3}	hole density at $x = 0$ and $t = 0$; $= N_0\ \alpha\ (1\text{-}R)\ \{1\text{-}R\ exp(-\alpha\ d)\}^{-1}$ where R(reflectivity) = 0.3 [16]

Since laser spot size is much larger than drift Epi layer thickness of d, a one-dimensional diffusion model can be utilized for the analysis. Just after the one single pulse is irradiated, the continuity equation of excess hole density $\Delta p(x,t)$ in the drift layer can be written as

$$\frac{\partial \Delta p(x,t)}{\partial t} = D_a \frac{\partial^2 \Delta p(x,t)}{\partial x^2} - \frac{\Delta p(x,t)}{\tau_b}, \qquad (A1)$$

where the drift Epi bulk lifetime τ_b, calculated from $Z_{1/2}$ defect density, is assumed to be uniform along x axis throughout the drift layer, and D_a is ambipolar diffusion coefficient [19]. The initial hole density profile immediately after the wafer is irradiated with pulsed light is expressed as follows.

$$\Delta p(x,0) = g_0 \exp(-\alpha x). \qquad (A2)$$

The flow of excess holes into the surface or into the drift/buffer interface is expressed by the boundary conditions.

$$D_a \frac{\partial \Delta p(0,t)}{\partial x} = S_0 \Delta p(0,t), \quad (A3)$$

$$D_a \frac{\partial \Delta p(d,t)}{\partial x} = -S_d \Delta p(d,t), \quad (A4)$$

where S_0 is the surface recombination velocity and S_d is the drift/buffer interface recombination velocity. The general solution of Eq. *A*1 is given by the Fourier series.

$$\Delta p(x,t) = \sum_{n=1}^{\infty} \Gamma_n \Phi_n(x) F_n(t). \quad (A5)$$

Here $\Phi_n(x)$ are spatial functions, $F_n(t)$ are time-dependent terms, and Γ_n are the time- and space-independent terms. From the boundary condition *A*3 and *A*4, let $S_a = S_0/D_a$ and $S_b = S_d/D_a$, then

$$\Phi_n(x) = a_n \cos(a_n x) + S_a \sin(a_n x), \quad (A6)$$

and

$$\cot(a_n d) = \frac{1}{(S_a + S_b)} \left(a_n - \frac{S_a S_b}{a_n} \right), \quad (A7)$$

are obtained, where a_n are solutions of the characteristic equation *A*7, and $F_n(t)$ are given by

$$F_n(t) = exp\left\{ -\left(\frac{1}{\tau_b} + a_n^2 D_a \right) t \right\}. \quad (A8)$$

Initial condition *A*2 and substituting $t = 0$ for *A*5 gives the Fourier series

$$\Delta p(x,0) = \sum_{n=1}^{\infty} \Gamma_n \Phi_n(x) = \mathrm{g}_0 \exp(-\alpha x), \quad (A9)$$

and solving it, we obtain

$$\Gamma_n = \frac{2\mathrm{g}_0 d}{\left\{ 1 + \left(\frac{a_n}{\alpha} \right)^2 \right\} \left[(a_n d)^2 + (S_a d)^2 + S_a d + S_b d \left\{ cos(a_n d) + \frac{S_a}{a_n} sin(a_n d) \right\}^2 \right] \times \left[\frac{a_n}{\alpha} \left\{ 1 - exp(-\alpha d) cos(a_n d) + \frac{a_n}{\alpha} exp(-\alpha d) sin(a_n d) \right\} + \frac{S_a}{\alpha} \left\{ \frac{a_n}{\alpha} - exp(-\alpha d) sin(a_n d) - \frac{a_n}{\alpha} exp(-\alpha d) cos(a_n d) \right\} \right]}. \quad (A10)$$

Accordingly, the average hole density $\Delta P(t)$ in the drift layer is given by integrating $\Delta p(x,t)$ of Eq. *A*5 with ranging from 0 to *d* and dividing by *d* into the following.

$$\Delta P(t) = \frac{1}{d} \sum_{n=1}^{\infty} \Gamma_n \Gamma'_n F_n(t), \quad (A11)$$

where, the coefficient Γ'_n is expressed as

$$\Gamma'_n = \frac{S_a}{a_n} + \frac{S_b(a_n^2 + S_a^2)sin(a_n d)}{a_n^2(S_a + S_b)}. \qquad (A12)$$

Because in Eq. $A11$, the surface and interface recombination velocities S_0 and S_d are unknown, but since the number of dangling bonds at the wafer surface is much larger than at the drift/buffer interface, in calculation of average hole density of the drift layer $\Delta P(t)$, the interface recombination velocity at the drift/buffer interface is assumed to be relatively small and fixed at S_d =100 cm s^{-1}, and surface recombination velocity is varied with S_0=1000, 2000, 5000, and 10000 cm s^{-1}.
As a result, as shown in Fig. A1, the peak value (t=0) of $\Delta P(t)$ with S_0 of 1000 to 10000 cm s^{-1} reaches 1.3× 10^{17} cm^{-3}, and the period during which $\Delta P(t)$ exceeds about 2.0× 10^{16} cm^{-3}, the literature value for the expansion threshold of 1SSF, is estimated to be 100 to 300 ns. Note that Eq. $A11$ is an infinite sum of exponential components with various time constants, but the value of Eq. $A11$ is mostly determined by the first mode component because the higher order terms have sharply smaller values. (Fig. A1 shows the summation of the first five terms (n=1-5).) In case of S_0 = 5000 cm s^{-1}, for example, as seen in Fig. A2, the Si(g) core moving duration is not limited to 10 ns of pulse irradiation but is estimated to last for about 150 ns even after the irradiation.
Thus, the correlation equation between current density and UV irradiation should be modified as Equation (1) in the main text.

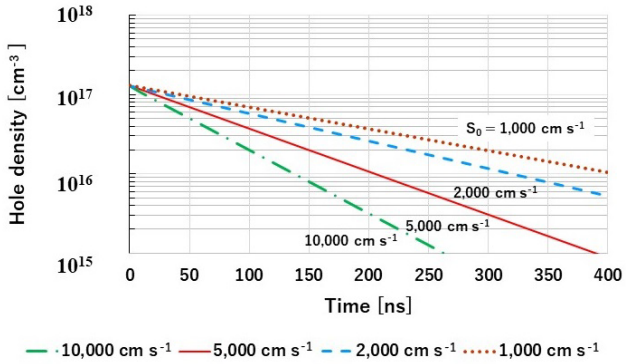

Fig. A1. Hole density decay profiles for different values of surface recombination velocity, S_0

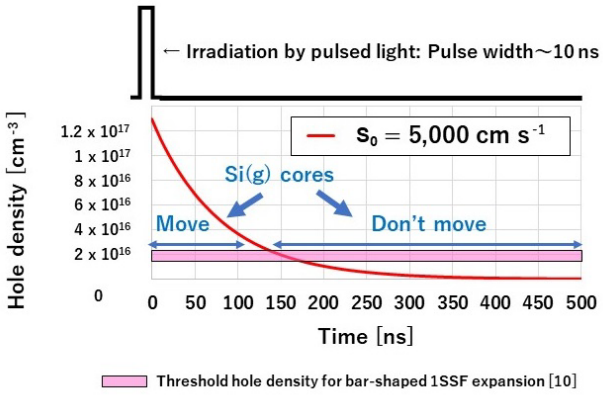

Fig. A2. Hole density decay profiles at S_0= 5,000 cm s^{-1} and real Si(g) core moving duration per one stimulation pulse

References

[1] M. Skowronski and S. Ha, J. Appl. Phys. 99, 011101 (2006).

[2] K. Maeda and S. Takeuchi, in *Dislocations in Solids*, ed. F. R. N. Nabarro and M. S. Duesbery, (Elsevier, Amsterdam, 1996), pp. 443.

[3] N. A. Mahadik, R. E. Stahlbush, M. G. Ancona, E. A. Imhoff, K. D. Hobart, R. L. Myers-Ward, C. R. Eddy, Jr., D. K. Gaskill, and F. J. Kub, Appl. Phys. Lett. 100, 042102 (2012).

[4] T. Tawara, T. Miyazawa, M. Ryo, M. Miyazato, T. Fujimoto, K. Takenaka, S. Matsunaga, M. Miyajima, A. Otsuki, Y. Yonezawa, T. Kato, H. Okumura, T. Kimoto, and H. Tsuchida, J. Appl. Phys. 120, 115101 (2016).

[5] S. Hayashi, T. Yamashita, J. Senzaki, T. Kato, Y. Yonezawa, K. Kojima, and H. Okumura, Appl. Phys. Express 12, 051007 (2019).

[6] K. Takano, Y. Igarashi, Mater. Sci. Forum 1062, 273 (2022).

[7] Y. Igarashi, K. Takano, Y. Matsushita, C. Shibata, Defect and Diffusion Forum 425, 75 (2023).

[8] Japan patent application number (2020) 03567

[9] K. Konishi, R. Fujita, K. Kobayashi, A. Yoneyama, K. Ishiji, H. Okino, A. Shima, T. Ujihara, AIP Advances 12, 035310 (2022).

[10] T. Tawara, S. Matsunaga, T. Fujimoto, M. Ryo, M. Miyazato, T. Miyazawa, K. Takenaka, M. Miyajima, A. Otsuki, Y. Yonezawa, T. Kato, H. Okumura, T. Kimoto, and H. Tsuchida, J. Appl. Phys. 123, 025707 (2018).

[11] S. G. Sridhara, Mater. Sci. and Eng. B61–62, 229 (1999).

[12] A. Galeckas, J. Linnros, V. Grivickas, U. Lindefelt, C. Hallin, Mater. Sci. Forum 264-268, 533 (1998)

[13] N. Watanabe, T. Kimoto, J. Suda, Jpn. J. Appl. Phy. 53, 108003 (2014).

[14] M. Bolou and D. Bois, J. Appl. Phys. 48, 4713 (1979).

[15] A. Usami and T. Kushida, "OYO BUTURI" 50, 607 (1981) (in Japanese).

[16] K. L. Luke and L. J. Cheng, J. Appl. Phys. 61, 2282 (1987).

[17] Y. Ogita, J. Appl. Phys., 79, 6954 (1996).

[18] S. Sumie, F. Ojima, K. Yamashita, K. Iba, and H. Hashizume, J. Electrochem. Soc. 152 G99 (2005).

[19] P. Grivickas, J. Linnros, and V. Grivickas, J. Mater. Res. 16, 524 (2001).